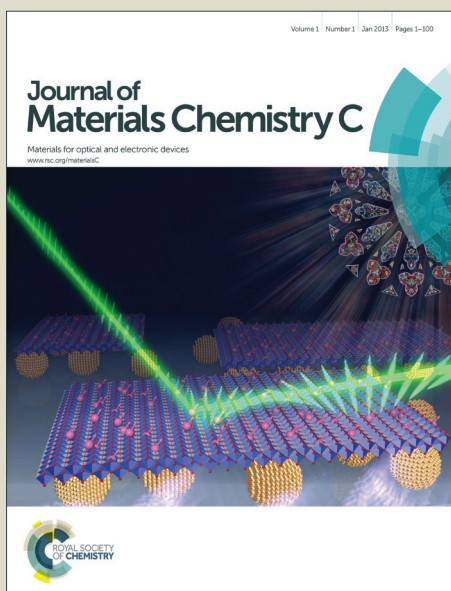


Journal of Materials Chemistry C

Accepted Manuscript



This is an *Accepted Manuscript*, which has been through the Royal Society of Chemistry peer review process and has been accepted for publication.

Accepted Manuscripts are published online shortly after acceptance, before technical editing, formatting and proof reading. Using this free service, authors can make their results available to the community, in citable form, before we publish the edited article. We will replace this *Accepted Manuscript* with the edited and formatted *Advance Article* as soon as it is available.

You can find more information about *Accepted Manuscripts* in the [Information for Authors](#).

Please note that technical editing may introduce minor changes to the text and/or graphics, which may alter content. The journal's standard [Terms & Conditions](#) and the [Ethical guidelines](#) still apply. In no event shall the Royal Society of Chemistry be held responsible for any errors or omissions in this *Accepted Manuscript* or any consequences arising from the use of any information it contains.

ARTICLE

Fabrication of pH- and temperature-directed supramolecular materials from 1D fiber to exclusively 2D planar structure by an ionic self-assembly approach

Cite this: DOI:
10.1039/x0xx00000x

Received 00th January 2012,
Accepted 00th January 2012

DOI: 10.1039/x0xx00000x

www.rsc.org

Yanjun Gong^a, Qiongzhen Hu^b, Ni Cheng^a, Tao Wang^c, Wenwen Xu^a, Yanhui Bi^a,

Li Yu^{a*}

Constructing multiple-response smart materials is a great interest and challenge for material science. Here we employed an ionic self-assembly (ISA) strategy to fabricate pH- and temperature-responsive supramolecular materials with controllable fluorescence emission properties by using charged Congo red (CR) and oppositely charged COOH-functionalized imidazolium-based surface active ionic liquid (SAIL), N-decyl-N'-carboxymethyl imidazolium bromide ([N-C₁₀, N'-COOH-Im]Br). One-dimensional (1D) slender fibers were obtained in aqueous solution at pH 3.2 by the self-assembly of CR/[N-C₁₀, N'-COOH-Im]Br (molar ratio =1:2) at room temperature. Noteworthy is that two-dimensional (2D) planar structures, viz. bamboo leaf-like, spindly, discoid and rectangular structures, were then formed only by further changing the pH of solution. Of particular interest is that the transition between 1D and 2D structures are pH reversible. We also found the slender fibers could aggregate into fiber bundle structures with the increasing temperature. In addition, fluorescence emission of the obtained 1D and 2D materials can be controlled by adjusting the morphologies of the aggregates. The electrostatic and hydrophobic interactions, in concert with π - π stacking between Congo red and [N-C₁₀, N'-COOH-Im]Br molecules were regarded as the main driving forces. The dimer-type π - π stacking existing among CR molecules was testified by DFT calculations.

Introduction

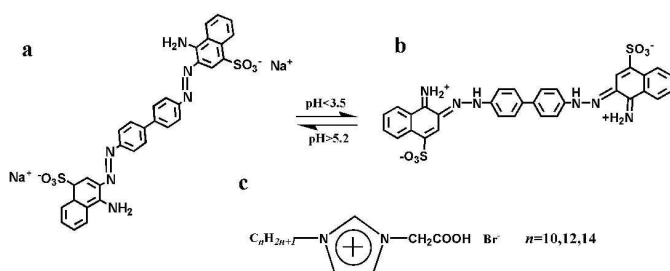
Supramolecular self-assembly avoiding complex organic synthesis has become one of the primary frontiers in materials science.¹⁻⁵ Functional self-assembled nanomaterials with well-defined shapes, sizes, and properties formed by organic small molecules are of great interest for applications in non-linear optical devices, electro-optical materials and light-energy conversion, etc.⁶ In particular, fluorescent switch behavior of the supramolecular materials has attracted considerable attention during recent years because it makes for promising optoelectronic devices. It is interesting but also challenging to find self-assembly systems which allow for controlling the shape and size of materials using an external stimulus such as temperature, light, pH or solvent.⁷⁻¹¹ For example,

controlling the transition of self-assembly from 1D fibers to exclusively 2D planar structures is rarely reported.

Ionic self-assembly (ISA)^{12,13} offers a potent and versatile route to prepare well-defined, discrete supramolecular architectures from simple molecular components under thermodynamic equilibrium. The strategy based on electrostatic interaction have made a great influence due to generalizability, simplicity and cheapness. Faul and Antonietti constructed supramolecular liquid crystal through complexation of N,N'-bis(ethylenetriethylammonium)perylene diimide and surfactant with opposite charges in water¹⁴. Wu et al. prepared onionlike hybrid assembled sphere by using ISA between surfactant and polyoxometalates¹⁵.

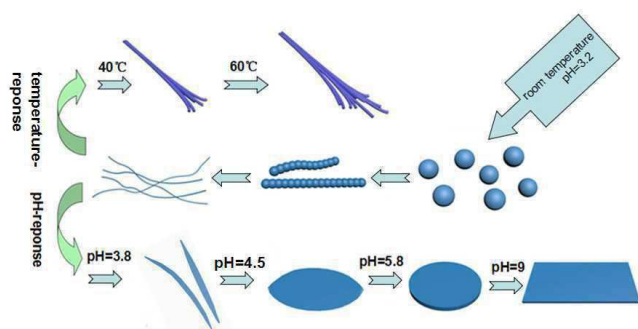
Surface active ionic liquids (SAILs), referred to the ionic liquids containing long alkyl chains which exhibit amphiphilic character, have emerged as a novel kind of amphiphiles. In recent years, various SAILs have been synthesized and the aggregates (e.g. micelles, gels, and lyotropic liquid crystal) formed by them have been widely investigated by some researchers^{16,17}, including our group¹⁸. It is demonstrated that compared to the traditional surfactants, they usually display superior surface-active properties and specific phase behavior in aqueous media. However, until now there are few reports using SAILs to prepare self-assembled supramolecular structures by ISA strategy.

Herein, we used an ISA strategy to produce pH- and temperature-sensitive supramolecular materials, which are capable of transforming 1D materials into 2D planar structures, with controllable fluorescence emission properties. The stimuli-responsive ISA complexes are consisted of charged Congo Red (CR) (Scheme 1a, b) units and oppositely charged COOH-functionalized imidazolium-based SAIL, N-decyl-N'-carboxymethyl imidazolium bromide ([N-C₁₀, N'-COOH-Im]Br) (Scheme 1c). Once upon a time, we reported that the aggregation behavior of [N-C₁₀, N'-COOH-Im]Br in aqueous solution. However, we did not use a ISA strategy to build response materials.



Scheme 1 The chemical structures of Congo Red at pH>5.2 (a) and pH<3.5 (b), and [N-C_n, N'-COOH-Im]Br (*n*=10, 12, 14) (c).

Slender fibers were observed for CR/[N-C₁₀, N'-COOH-Im]Br (molar ratio =1:2) in pH 3.2 aqueous solution at room temperature.



Scheme 2 Schematic showing the possible model for temperature- and pH-response of the supramolecular materials.

At elevated temperature, the slender fibers could be bundled due to the interdigitation between the hydrophobic domains on the fibers via hydrophobic interactions. In addition, by changing the pH of the aqueous solution, other various morphologies, including bamboo leaf-like, spindly, discoid and rectangular 2D assemblies were obtained. The changes of fluorescence for nanomaterials based on pH between “on” and “off” states are significant in solution. At the same time, the fluorescence emission could also be controlled by adjusting the morphologies of the aggregates.

Experimental Section

Materials

Congo red (99%) was purchased from J&K Chemical Technology, China. 1-bromododecane (98%), 1-bromododecane (98%), 1-bromotetradecane (98%), N-alkylimidazole (99%) and bromoacetic acid (99%) were bought from Aladdin Chemistry Co., Ltd. of China. Benzophenone (chemical pure) was obtained from Sinopharm Chemical Reagent Co., Ltd. All the above reagents were used without further purification. Triply distilled water was used in all the solutions.

Synthesis

COOH-functionalized imidazolium SAILs⁴³ were prepared as improved procedures according to our previous report⁴⁴. N-alkylimidazole was prepared as described previously. Bromoacetic acid (86 mmol) was added to 50 mL methanol solution of N-alkylimidazole (95 mmol) under the continuous stirring. The mixture was refluxed at 70 °C for 6 h under the protection of nitrogen. After methanol was removed, the residue was recrystallized five times from methanol/ether to obtain [N-C_n, N'-COOH-Im]Br (20 g, 63% yields). The chemical structures were ascertained by ¹H NMR spectroscopy with a Bruker Avance 300 spectrometer. And the ¹H NMR peak of D₂O (δ=4.70 ppm) was used as the reference in determining the proton chemical shifts for [N-C_n, N'-COOH-Im]Br. For [N-C₁₀, N'-COOH-Im]Br, ¹H NMR (D₂O, ppm): δ=8.80 (s, 1 H, CH), 7.46 (d, 1 H, CH), 7.46 (d, 1 H, CH), 4.88 (s, 2 H, CH₂), 4.18 (t, 2 H, CH₂), 1.83 (m, 2 H, CH₂), 1.27 (m, 14 H, CH₂), 0.80 (t, 3 H, CH₃).

Preparation of supramolecular structures

Aqueous solutions of CR (10 mL, 0.5 mM) and [N-C₁₀, N'-COOH-Im]Br (10 mL, 1 mM) were mixed and stirred in a 50 mL flask. After additional stirring for different time, the mixture was placed in a thermostatic water bath with the uncertainty of within ±0.1 °C. The obtained products were collected by filtration, washed three times with water to remove salts and possible precursors. The final products were dried under vacuum at 55 °C for 24 h.

Characterizations of supramolecular structures

The sizes and morphologies of supramolecular materials were characterized by scanning electron microscopy (SEM, JEOL JSM-7600F) operated at 5.0 kV. The samples were prepared by placing a drop of supramolecular aggregates in water onto a silicon wafer.

The nanostructures were characterized by transmission electron microscopy (TEM) (JEM-100CX II (JEOL)). The morphologies of samples were also characterized by a polarized optical microscope (POM) equipped with a charge-coupled device camera (Panasonic Super Dynamic II WVCP460).

The ¹H NMR spectra were recorded using a Bruker AV-300 NMR spectrometer with a pulse field gradient module (Z-axis) and a 5 mm sample tube. The instrument was operated at a frequency of 300.13 MHz at 25 °C with tetramethylsilane as an internal reference. Deuterated dimethylsulfoxide (DMSO) was selected as the solvent.

AFM images were collected in air under ambient conditions using the tapping mode with a NanoscopeIII/Bioscope scanning probe microscope from digital instruments.

UV/Vis spectra were measured in a quartz cell (light path of 1 cm) by using a HP 8453E instrument.

Small angle X-ray scattering (SAXS) measurements were performed using an Anton-paar SAX Sess mc² system with a Ni-filtered Cu K α radiation (1.54 Å) operated at 50 kV and 40 mA. The solid samples were placed in a stainless steel tank sealed by an aluminum foil. The distance from sample to detector was 264.5 mm.

Fourier transform IR (FTIR) spectra were recorded between 4000 and 400 cm⁻¹ by using a VERTEX-70/70v FTIR spectrometer (Bruker Optics, Germany) on pressed thin KBr disks of samples.

Results and discussion

For CR/[N-C₁₀, N'-COOH-Im]Br system, the morphologies of supramolecular materials formed at a molar ratio of 1:2 in pH 3.2 aqueous solution at room temperature were examined by transmission electron microscopy (TEM). As shown in Fig. 1a, slender fibers with an average width of ca. 100 nm were prepared after 4 h. Fig. S1a shows a typical AFM image of the slender fibers self-assembled by CR/[N-C₁₀, N'-COOH-Im]Br. Surprisingly, AFM image and phase image (Fig. S1b) present that nanoparticles orient themselves to fuse and then form 1D fiber structures to decrease the surface energy¹⁹⁻²¹, where dispersed and individual nanoparticles can still be observed. With increasing time to 12 h, slender fibers could aggregate into feather-like materials with 0.5–1 μm in width (Fig. 1b). When prolonged to 48 h, the feather-like structures of 3 μm in width were observed (Fig. 1c). It is obvious that either the narrow or wide feather-like supramolecular materials were assembled by individual slender fibers²². Meanwhile, a time-dependent color change in the aqueous solution was observed by the naked eye (Fig. 1d). A characteristic red emission was observed for these materials after irradiation, indicating their fluorescent properties (Fig. 3a). To further study the aggregation of CR/[N-C₁₀, N'-COOH-Im]Br with aging, variable-time UV-Vis experiments were performed (Fig. S2). The absorption bands are around 530 nm and 567 nm (n-π*), respectively, which are the characteristic absorption peaks of the chromophore. With the extension of time, the absorption intensity of all the major bands decreases remarkably. When the time exceeded to 24 h, a new shoulder peak was observed at approximately 740 nm, demonstrating the occurrence of a new aggregation^{23,24}.

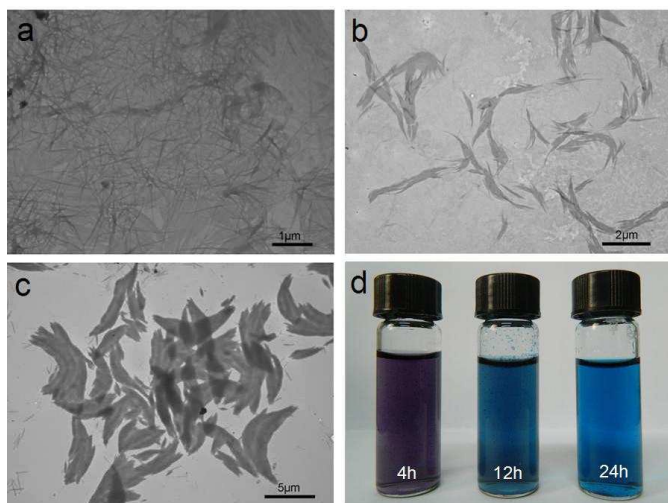


Fig. 1 TEM images of supramolecular structures formed by CR/[N-C₁₀, N'-COOH-Im] Br (molar ratio=1:2) in pH 3.2 aqueous solution

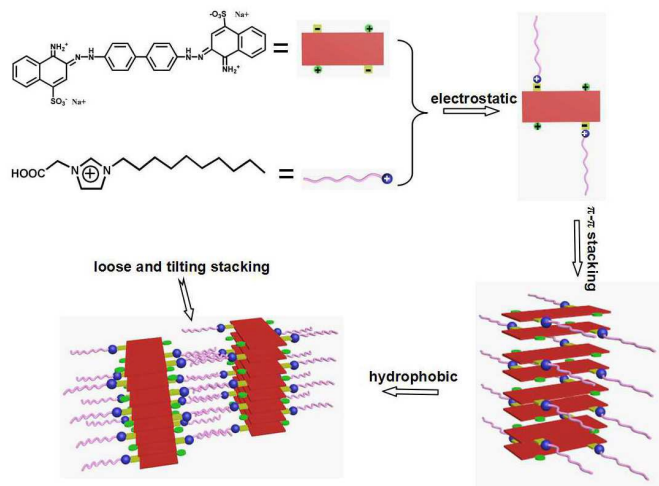
at room temperature after 4 h (a), 12 h (b), and 24 h (c); the photos of CR/[N-C₁₀, N'-COOH-Im]Br solution at different time (d).

To understand how these highly ordered materials are formed by using the ISA strategy, their composition was investigated first. As is shown in Fig. S3, all proton signals of CR and [N-C₁₀, N'-COOH-Im]Br molecules in the nanofibers prepared in pH 3.2 aqueous solution were obviously observed. The stoichiometry of these two molecules in the supramolecular materials is proved to be 1:2 by comparing the peak integral intensities²⁵. The electrostatic interaction between CR and [N-C₁₀, N'-COOH-Im]Br molecules was confirmed by FTIR pattern (Fig. S4). FTIR band of CR molecule at 1058 cm⁻¹ corresponds to the vibrations of sulfonic groups. After the formation of materials, this peak shifts from 1058 to 1039 cm⁻¹, which can be ascribed to the existence of electrostatic interaction¹⁵. To further investigate the π-π stacking during process of the supramolecular self-assembly, UV-Vis absorption spectra of CR and CR/[N-C₁₀, N'-COOH-Im]Br samples in pH 3.2 aqueous solution were obtained (Fig. S5). The strong absorption of CR molecules occurs around 570 nm (n-π*). For the slender fibers, the maximum absorption is blue-shifted by 30 nm and is significantly reduced, which can be ascribed to the π-π stacking aroused by the supramolecular self-assembly of CR and [N-C₁₀, N'-COOH-Im]Br molecules^{26,27}. The shift of the maximum absorption in the UV-Vis spectra is typical for the parallel arrangement of chromophore dipoles (H-aggregation)²⁸. SAXS diffractogram (Fig. S6) shows two scattering peaks, indicative of the highly ordered supramolecular structures. The calculated interplanar distance (*d*) of the typical lamellar structure is 1.39 nm. The ratio of the two peaks is 1:2, suggesting a typical lamellar structure of nanoparticles. The energy minimized structures of [N-C₁₀, N'-COOH-Im]Br and CR molecules are shown in Fig. S7, which demonstrates that the hydrophobic chain length of [N-C₁₀, N'-COOH-Im]Br is 1.36 nm. The width of CR is 0.61 nm. Thus the theory of layer spacing is 1.66 nm. Apparently, the layer spacing of experiment is less than that of theory. It may be originated from the loose stacking and tilting stacking of [N-C₁₀, N'-COOH-Im]Br molecules in the theoretical calculation²⁹. At the same time, frequencies for the antisymmetric ν_{as}(CH₂) and the symmetric stretching ν_s(CH₂) bands are sensitive to the conformation of the alkyl chains. When the alkyl chain are highly ordered (all-trans conformation), the bands appear near 2918 and 2850 cm⁻¹, respectively. However, when they are arranged in a poor orderly way, the frequencies may shift to higher bands and the gauche conformation will increase. In the FTIR spectra (Fig. S4) of the complex, the ν_{as}(CH₂) and ν_s(CH₂) bands appear around 2922 and 2851 cm⁻¹, respectively, the hydrocarbon chains stack loosely³⁰. This result is consistent with that of SAXS.

To explore the role of hydrophobic interaction provided by the hydrophobic chain of SAIL playing in the formation of supramolecular structures, we changed the hydrophobic chain length of SAIL and synthesized [N-C_{*n*}, N'-COOH-Im]Br (*n*=12, 14) (Scheme 1c). When [N-C₁₀, N'-COOH-Im]Br was replaced by [N-C₁₂, N'-COOH-Im]Br, aquatic plant-like materials were generated (Fig. S8). As for [N-C₁₄, N'-COOH-Im]Br, only irregular precipitates appeared. These phenomena prove that only appropriate hydrophobic effect can contribute to the fabrication of 1D slender fibers. An increase in the hydrophobic chain length can result in the enhancement of the hydrophobic interaction. Consequently, the aggregates tend to grow to reduce the chain's contact area with water³¹. Therefore, during the formation of supramolecular fibers, the appropriate hydrophobic chain length of [N-C₁₀, N'-COOH-Im]Br molecule plays a crucial role in the modification of effective molecular stacking and unique morphology formation.

In order to obtain a better insight into the assembly mechanism of CR/[N-C₁₀, N'-COOH-Im]Br, we attempted to carry out computational studies on small aggregates, which are the probable building units for the larger molecular aggregates by the dispersion-corrected semiempirical PM7 method³². Firstly, We optimized the geometries of the dimeric (C2) at the level of ω B97X-D/6-31G(d,p)³³. In the preliminary models, we chose two CRs and four counters to model this aggregation. Here, for computational convenience, we replaced the longer hydrophobic chains by methyl groups. Noncovalent weak interactions, such as hydrogen bonding, electrostatic interaction or π - π stacking are satisfactorily captured by ω B97X-D/6-31G(d,p). Hence it is an ideal choice for predicting the stability of dimeric (C2). As is shown in Fig.S9, CR molecule and two [N-C₁₀, N'-COOH-Im]Br molecules can be connected by electrostatic interaction. The CR dimers exhibits an interplanar distance between the two aromatic rings is 3.48Å, indicative of π - π stacking (face-to-face stacking), viz. H-aggregates³⁴. This has also been supported by the experimental results of UV-Vis measurements. Then we also expanded our investigations by energy minimization of the original monomer and larger aggregates comprising of six CRs and twelve [N-C₁₀, N'-COOH-Im]Br. The calculated interplanar distance between the two aromatic rings is 3.56Å (Fig.S10). Obviously, PM7 method also predicts C2 dimers formed by π - π stacking with comparable stability^{35,36}.

Based on the above results, structural models can be proposed to explain the formation of these materials, as illustrated in Scheme 3. To begin with, CR and [N-C₁₀, N'-COOH-Im]Br molecules can self-assemble into building block by electrostatic interaction. Next, the building block associates through π - π stacking, leading to the formation of "H-type" aggregates. Hydrophobic interaction can make a larger aggregation. Eventually, supramolecular materials can be formed by electrostatic interaction, π - π stacking and Hydrophobic interaction.



Scheme 3 The possible model for the self-assembly of CR/[N-C₁₀, N'-COOH-Im]Br.

To clarify the structural changes upon the pH stimulus, examinations of CR/[N-C₁₀, N'-COOH-Im]Br supramolecular materials assembled at other pH (3.5, 3.8, 4.5, 5.8 and 9.0) were carried out by TEM, scanning electron microscopy (SEM) and polarizing optical microscopy (POM). The results reveal an interesting morphology evolution with pH for the assembled materials from 1D fibers to 2D planar structures. As presented above, slender fibers (Fig.1a) in the aqueous solution at pH 3.2 were

fabricated via the self-assembly of CR and [N-C₁₀, N'-COOH-Im]Br molecules. It is noted that, only a slight increase at pH 3.5, bamboo leaf-like 2D planar structures were observed in the SEM (Fig. 2a) and TEM (Fig. S11a) image, respectively. At pH 3.8, slender fibers absolutely disappeared and completely transformed into bamboo leaf-like structures (Fig. S11b). Fig. 2b demonstrates that bamboo leaf-like structures are consisted of free fibrils. As the pH of solution was increased to 4.5, uniform spindle-shaped supramolecular materials were obtained (Fig. 2c). In the aqueous solution at pH 5.8, discoid-like structures with a diameter of about 20 μ m were observed (Fig. 2d). At pH 9.0, the discoid-to-rectangle shape transition occurred (Fig.2e). Both the macroscopic discoid- and rectangle-shaped supramolecular structures show strong birefringence (Fig. S12). It is also noteworthy that slender fibers could be rebuilt when pH of solution turned back to 3.2 (Fig.S13). The pH-dependent series transformation of the assembled structures can be attributed to the different protonation states of CR and [N-C₁₀, N'-COOH-Im]Br in various pH aqueous solutions. This can be detected by UV-Vis absorption and ¹HNMR spectra. As depicted in Fig. 2f, when the pH in solution is changed from 3.2 to 3.8, UV-Vis absorption spectra exhibit a slight blue shift and the intensity of absorption is reduced, which can affect the electrostatic interaction and π - π packing between CR molecules. With the change of pH from 3.5 to 4.5. UV-Vis absorption spectra exhibit a strong blue shift and the intensity of absorption is reduced. At the same time, a shoulder peak is observed at approximately 600 nm, which can suggest the CR molecule undergoes a transformation from quinoid to azobenzene structure. When the pH increases to 5.8, the shoulder peak around 600 nm disappears, which indicates the CR molecule has completely turned into azobenzene structure (Scheme 1a). What's more, simultaneously, ¹HNMR spectra (Fig. S14) show that the CR/[N-C₁₀, N'-COOH-Im]Br material composition has changed into 1:1. The reduction of hydrophobic chains lead to formation of micrometer materials. When the pH changes into 9.0, ¹HNMR spectra (Figure. S15) present the composition of CR and [N-C₁₀, N'-COOH-Im]Br is 1:1. At the same time, we optimized the aggregation between two CRs and two counters using ω B97X-D/6-31G(d,p) (Fig.S16). The CR dimers exhibits an interplanar distance between the two aromatic rings is 3.52Å, indicative of π - π stacking (face-to-face stacking). As reported, the isoelectric point (PI) of [N-C₁₀, N'-COOH-Im]Br is 6.5³⁷. Therefore, as pH increases from 5.8 to 9.0, the COOH group of [N-C₁₀, N'-COOH-Im]Br molecule turns into COO⁻, indicating the original cationic amphiphile converts into zwitterion. Thus, the electrostatic repulsive interaction between CR and [N-C₁₀, N'-COOH-Im]Br molecules appears at pH 9.0. This can be supported by the ¹HNMR spectra of CR/[N-C₁₀, N'-COOH-Im]Br complex and pH 9.0, respectively (Fig. S17). The signal of the methene on the carboxymethyl of [N-C₁₀, N'-COOH-Im]Br shifts obviously, which can be ascribed to the changes of electrostatic interaction as a result of deprotonation of [N-C₁₀, N'-COOH-Im]Br molecule.³⁸ But the electrostatic repulsive interaction can not separate CR and [N-C₁₀, N'-COO⁻-Im]Br molecules and can only influence π - π stacking between two CRs molecules. The interplanar distance between the two aromatic rings has a change from 3.52Å to 3.68Å (Fig.S18). Furthermore, the fluorescence emission of the 1D and 2D materials can be controlled by adjusting the morphologies of the aggregates (Fig. 3). The fluorescence spectral changes of nanomaterials in solution are presented in Fig. S19. When pH=9.0, there exists a strong peak around 635 nm. When pH change into 3.2, the peak of 635 nm disappears and the peak of 830 nm appears. Fluorescence switching of nanomaterials based on the change of pH was performed for numerous times in solution. The nanomaterials present relatively good fluorescence switching on-off property (Fig. 4).

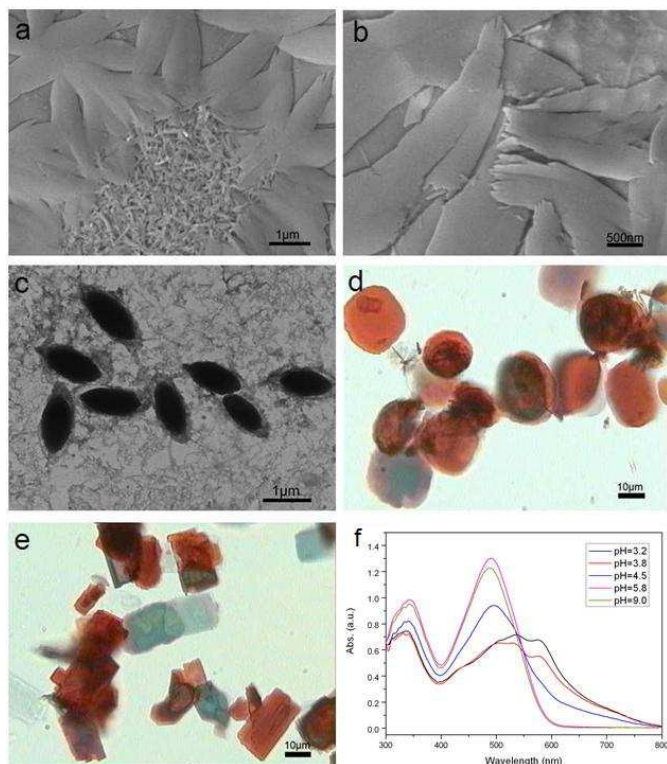


Fig. 2 SEM (a, b), TEM (c) and POM images (d, e) of CR/[N-C₁₀, N'-COOH-Im]Br assembled materials at room temperature in aqueous solutions with different pH: 3.5 (a), 3.8 (b), 4.5 (c), 5.8 (d) and 9.0 (e). pH-dependent UV/Vis absorption spectra of CR/[N-C₁₀, N'-COOH-Im]Br complex at room temperature (f).

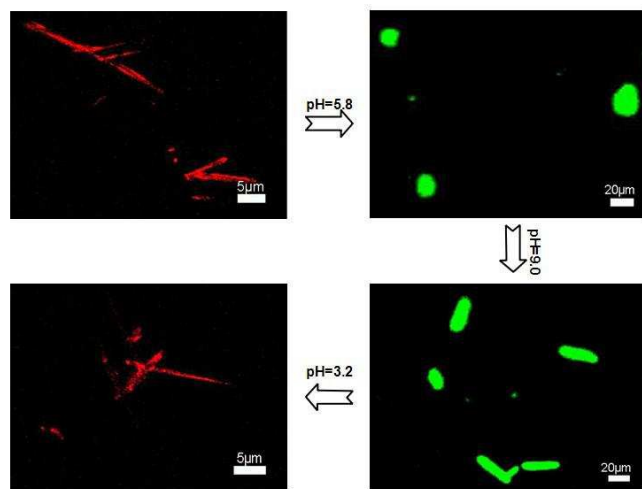


Fig. 3 Confocal fluorescence microscopy image of supramolecular materials formed by CR and [N-C₁₀, N'-COOH-Im]Br (molar ratio=1:2) in pH 3.2 (a), 5.8 (b) and 9.0 (c) aqueous solution at room temperature. Confocal fluorescence microscopy image of CR/[N-C₁₀, N'-COOH-Im]Br assembled materials reversed at pH 3.2 (d).

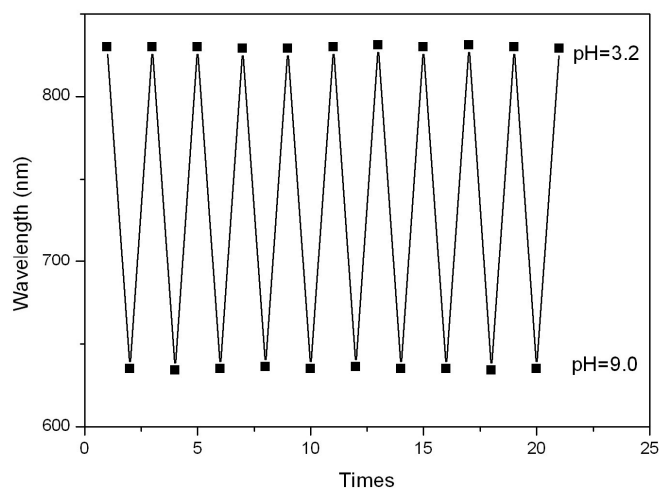


Fig. 4 Fluorescence switching on-off cycles of nanomaterials in pH=3.2 and 9.0 aqueous solution.

To study the temperature response of the supramolecular materials, temperature-controlled self-assembly experiments for CR/[N-C₁₀, N'-COOH-Im]Br (molar ratio=1:2) solutions at pH 3.2 were performed. Upon increasing the temperature to 40 °C, the mixture of CR and [N-C₁₀, N'-COOH-Im]Br produced the thick fibers with ~0.2 μm (Fig. 5a). Incubating the mixture at 60 °C accelerated thick fibers clustering, leading to reduction in the free fibers fraction and formation of bigger fiber bundles with approximate 0.3~0.4 μm (Fig. 5b). Interestingly, we captured the TEM image of intermediate structures which further aggregated into fiber bundles. As reported³⁹, the above observed profound effect of temperature on the supramolecular structures can be ascribed to the changes of short-range attraction, which is most probably of entropic origin. When the temperature increases from room temperature to 40 °C or 60 °C, the solvophobic interactions of hydrophobic domains on the surface of the slender fibers are enhanced. It leads to the shielding of the hydrophobic patches from the surrounding polar medium, which then enables and facilitates the interdigitation between the hydrophobic parts via hydrophobic interactions, resulting in bundling of the slender fibers⁴⁰. The temperature-dependent self-assembly of CR and [N-C₁₀, N'-COOH-Im]Br in aqueous solution can also be revealed by the UV-Vis spectroscopic investigation (Fig. S20). At room temperature, for CR/[N-C₁₀, N'-COOH-Im]Br complex, the absorption bands are around 530 nm and 567 nm ($n-\pi^*$), which are the characteristic absorption peaks of the chromophore. The absorption band at about 330 nm belongs to the electronic $\pi-\pi^*$ transition superimposed with vibrational transitions. With the increasing temperature up to 40 °C or 60 °C, there is only a slight change in the absorbance around 330 nm. However, the absorption of embedded chromophore exhibits a significant shift. Moreover, the shoulder peak is not detectable. These phenomena suggest that temperature-induced fibers aggregation can exert an effect on the chromophore of CR/[N-C₁₀, N'-COOH-Im]Br complex^{41,42}.

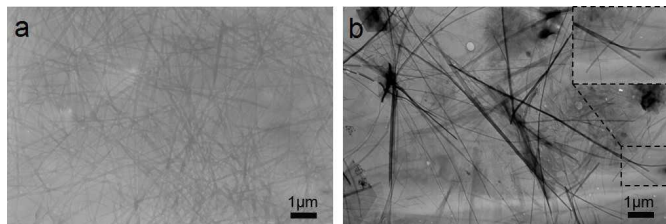


Fig. 5 TEM images of CR/[N-C₁₀, N'-COOH-Im]Br supramolecular structures in the aqueous solution at pH 3.2 after 4 h at different temperature, 40 °C (a), 60 °C (b). The inset in b is the magnified TEM image of the selected fiber bundles.

Conclusions

Based on ISA strategy, supramolecular materials were generated from CR and oppositely charged COOH-functionalized imidazolium-based SAIL, [N-C₁₀, N'-COOH-Im]Br. Dual-stimulus (temperature and pH) induced structure transformation of CR/[N-C₁₀, N'-COOH-Im]Br was observed. The fabricated supramolecular materials shown 1D slender fibers were obtained via self-assembly in aqueous solution at pH 3.2 and room temperature. Of particular interest is that 2D planar structures, viz. bamboo leaf-like, spindly, discoid and rectangular structures. This can be attributed to the hydrophobic interaction depending on temperature and different protonation states of CR and [N-C₁₀, N'-COOH-Im]Br molecules related to the pH of aqueous solutions. Noteworthy is that the transition between 1D and 2D structures are pH reversible. In addition, these supramolecular fibers also manifest superior fluorescent properties. The fabrication of the self-assembled structures is considered to base on the electrostatic and hydrophobic interactions, cooperative with the π - π stacking. DFT calculations prove that the dimeric entities of CR molecules are energetically favorable due to an intermolecular π - π stacking interaction, which contributes significantly to the resulting aggregates. This work provides an important clue in the achievement of fluorescence emission inversion in supramolecular materials with different dimensions only by choosing appropriate temperature or pH, which may have potential application in optoelectronics and fast switching.

Acknowledgements

This work was supported by the National Natural Science Foundation of China (No. 21373128), Scientific and Technological Projects of Shandong Province of China (No. 2014GSF117001), the Natural Science Foundation of Shandong Province of China (No. ZR2011BM017) and the Project of Sinopec (No. P13045).

Notes and references

^aKey Laboratory of Colloid and Interface Chemistry, Shandong University, Ministry of Education, Jinan 250100, PR China.

^bDepartment of Chemistry, University of Houston, Houston 77204, United States.

^c Production Technology Institute, Shengli Oilfield, Dongying, 257000, PR China.

Electronic Supplementary Information (ESI) available: [details of any supplementary information available should be included here]. See DOI: 10.1039/b000000x/

References

1. M. Grzelczak, J. Vermant, E. M. Furst and L. M. Liz-Marzán, *ACS Nano*. **2010**, 4, 3591-3605.
2. V. Sashuk, K. Winkler, A. Żywociński, T. Wojciechowski, E. Górecka and M. Fiałkowski, *ACS Nano*. **2013**, 7, 8833-8839.
3. S. I. Stupp, V. LeBonheur, K. Walker, L. S. Li, K. E. Huggins, M. Keser and A. Amstutz, *Science*. **1997**, 276, 384-389.
4. P. Jonkheijm, P. van der Schoot, A. P. Schenning and E. W. Meijer, *Science*. **2006**, 313, 80-83.
5. J. D. Hartgerink, E. Beniash and S. I. Stupp, *Science*. **2001**, 294, 1684-1688.
6. Y. Huang, Y. Yan, B. M. Smarsly, Z. Wei and C. F. J. Faul, *J. Mater. Chem.* **2009**, 19, 2356-2362.
7. S. Lee, S. Oh, J. Lee, Y. Malpani, Y.-S. Jung, B. Kang, J. Y. Lee, K. Ozasa, T. Isoshima, S. Y. Lee, M. Hara, D. Hashizume and J.-M. Kim, *Langmuir*. **2013**, 29, 5869-5877.
8. K. Liu, Y. Yao, Y. Kang, Y. Liu, Y. Han, Y. Wang, Z. Li and X. Zhang, *Sci. Rep.* **2013**, 3, 2372.
9. C. Wang, Q. Chen, H. Xu, Z. Wang and X. Zhang, *Adv. mater.* **2010**, 22, 2553-2555.
10. M. C. P. Wang, X. Zhang, E. Majidi, K. Nedelec and B. D. Gates, *ACS Nano*. **2010**, 4, 2607-2614.
11. X. Zhang, J. Zou, K. Tamhane, F. F. Kobzeff and J. Fang, *Small*. **2010**, 6, 217-220.
12. M. Zhao, Y. Zhao, L. Zheng and C. Dai, *Chem. Eur. J.* **2013**, 19, 1076-1081.
13. C. F. J. Faul and M. Antonietti, *Adv. mater.* **2003**, 15, 673-683.
14. A. Laiho, B. M. Smarsly, C. F. J. Faul and O. Ikkala, *Adv. Funct. Mater.* **2008**, 18, 1890-1897.
15. H. Li, H. Sun, W. Qi, M. Xu and L. X. Wu, *Angew. Chem.* **2007**, 1300-1303.
16. N. Cheng, Q. Hu, Y. Bi, W. Xu, Y. Gong and L. Yu, *Langmuir*. **2014**, 30, 9076-9084.
17. P. D. Galgano and O. A. El Seoud, *J. Colloid. Interf. Sci.* **2010**, 345, 1-11.
18. J. Jiao, B. Dong, H. Zhang, Y. Zhao, X. Wang, R. Wang and L. Yu, *J. Phys. Chem. B.* **2011**, 116, 958-965.
19. V. J. Anderson and H. N. W. Lekkerkerker, *Nature*. **2002**, 416, 811-815.
20. K.-S. Cho, D. V. Talapin, W. Gaschler and C. B. Murray, *J. Am. Chem. Soc.* **2005**, 127, 7140-7147.
21. Y. Min, M. Akbulut, K. Kristiansen, Y. Golan and J. Israelachvili, *Nat Mater.* **2008**, 7, 527-538.

22. Y.-C. Lin, E. J. Petersson and Z. Fakhraei, *ACS Nano*. **2014**.
23. N. Houbenov, A. Nykänen, H. Iatrou, N. Hadjichristidis, J. Ruokolainen, C. F. J. Faul and O. Ikkala, *Adv. Funct. Mater.* **2008**, 18, 2041-2047.
24. J. Hu, W. Kuang, K. Deng, W. Zou, Y. Huang, Z. Wei and C. F. J. Faul, *Adv. Funct. Mater.* **2012**, 22, 4149-4158.
25. Y. Guan, M. Y. Zakrevskyy, J. Stumpe, M. Antonietti and C. F. J. Faul, *Chem. Commun.* **2003**, 894-895
26. U. Rösch, S. Yao, R. Wortmann and F. Würthner, *Angew. Chem.* **2006**, 118, 7184-7188.
27. Y. Zakrevskyy, J. Stumpe and C. F. J. Faul, *Adv. Mater.* **2006**, 18, 2133-2136.
28. G. Lu, Y. Chen, Y. Zhang, M. Bao, Y. Bian, X. Li and J. Jiang, *J. Am. Chem. Soc.* **2008**, 130, 11623-11630.
29. T. R. Zhang, W. Teng, Y. Q. Fu, R. Lu, *J. Mater. Chem.* **2002**, 12, 1453-1458.
30. T. Zhang, C. Spitz, M. Antonietti and C. F. J. Faul, *Chem. Eur. J.* **2005**, 11, 1001-1009.
31. X.-h. Cheng, Y. Peng, C. Gao, Y. Yan and J.-b. Huang, *Colloid. Surfaces. A* **2013**, 422, 10-18.
32. J. J. P. S. MOPAC2012, Stewart Computational Chemistry, Version 12.365L.
33. R. A. Gaussian 09, M. J. Frisch, G. W. Trucks, H. B. Schlegel, G. E. Scuseria, M. A. Robb, J. R. Cheeseman, G. Scalmani, V. Barone, B. Mennucci, G. A. Petersson, H. Nakatsuji, M. Caricato, X. Li, H. P. Hratchian, A. F. Izmaylov, J. Bloino, G. Zheng, J. L. Sonnenberg, M. Hada, M. Ehara, K. Toyota, R. Fukuda, J. Hasegawa, M. Ishida, T. Nakajima, Y. Honda, O. Kitao, H. Nakai, T. Vreven, J. A. Montgomery, J. J. E. Peralta, F. Ogliaro, M. Bearpark, J. J. Heyd, E. Brothers, K. N. Kudin, V. N. Staroverov, R. Kobayashi, J. Normand, K. Raghavachari, A. Rendell, J. C.; Iyengar, S. S.; Tomasi, J.; Cossi, M.; Rega, N. Burant, J. M. Millam, M. Klene, J. E. Knox, J. B. Cross, V. Bakken, C. Adamo, J. Jaramillo, R. Gomperts, R. E. Stratmann, O. Yazyev, A. J. Austin, R. Cammi, C. Pomelli, J. W. Ochterski, R. L. Martin, K. Morokuma, V. G. Zakrzewski, G. A. Voth, P. Salvador, J. J. Dannenberg, S. Dapprich, A. D. Daniels, O. Farkas, J. B. Foresman, J. V. Ortiz, J. Cioslowski, and D. J. Fox, Inc. Gaussian, Wallingford CT, 2009.
34. M. T. Fenske, W. Meyer-Zaika, H.-G. Korth, H. Vieker, A. Turchanin and C. Schmuck, *J. Am. Chem. Soc.* **2013**, 135, 8342-8349.
35. M. Korth, M. Pitoňák, J. Řezáč and P. Hobza, *J. Chem. Theory. Comput.* **2009**, 6, 344-352.
36. M. R. Molla, D. Gehrig, L. Roy, V. Kamm, A. Paul, F. Laquai and S. Ghosh, *Chem. Eur. J.* **2014**, 20, 760-771.
37. X. Wang, J. Liu, L. Yu, J. Jiao, R. Wang and L. Sun, *J. Colloid. Interf. Sci.* **2013**, 391, 103-110.
38. C. Wang, G. Wang, Z. Wang and X. Zhang, *Chem. Eur. J.* **2011**, 17, 3322-3325.
39. S. A. Semerzhiev, D. R. Dekker, V. Subramaniam and M. M. A. E. Claessens, *ACS Nano*. **2014**, 8, 5543-5551.
40. L. Li, Y. Che, D. E. Gross, H. Huang, J. S. Moore and L. Zang, *ACS Macro Letters*. **2012**, 1, 1335-1338.
41. G. Wu, J. Thomas, M. Smet, Z. Wang and X. Zhang, *Chem. Sci.* **2014**, 5, 3267-3274.
42. Y. Zakrevskyy, C. F. J. Faul, Y. Guan and J. Stumpe, *Adv. Funct. Mater.* **2004**, 14, 835-841.
43. J. C. Y. Lin, C.-J. Huang, Y.-T. Lee, K.-M. Lee and I. J. B. Lin, *J. Mater. Chem.* **2011**, 21, 8110-8121.
44. X. Wang, L. Yu, J. Jiao, H. Zhang, R. Wang and H. Chen, *J. Mol. Liq.* **2012**, 173, 103-107.